

# MULTI-SCALE AND MULTI-SENSOR APPROACHES FOR THE PROTECTION OF CULTURAL NATURAL HERITAGE: THE ISLAND OF SANTO SPIRITO IN VENICE

A. Martino <sup>1,2\*</sup>, F. Gerla <sup>1,3</sup>, C. Balletti <sup>1</sup>

<sup>1</sup> Laboratorio di Cartografia e GIS, Dipartimento di Culture del Progetto, Università IUAV di Venezia, Dorsoduro 1827, 30123 Venice, Italy – (amartino, fgerla, balletti)@iuav.it

<sup>2</sup> Dipartimento di Ingegneria e Architettura, Università degli studi di Trieste, Via Alfonso Valerio 6/1, 34127 Trieste, Italy – andrea.martino@phd.units.it

<sup>3</sup> Dipartimento di Ingegneria Civile, Edile e Ambientale, Sapienza Università di Roma, Via Eudossiana, 18, 00184 Roma, Italy – federica.gerla@uniroma1.it

**KEY WORDS:** Cultural Natural Heritage, 3D survey, Copernicus Sentinel, UAV, TLS, data integration.

## ABSTRACT:

The study of Cultural Natural Heritage (CNH) requires the development of multi-disciplinary and multi-scale methodologies for data recording, representation, and correlation from various platforms such as terrestrial, aerial and satellite sensors. The heterogeneity of geo-databases currently available demands on-site validation and time monitoring to control the phenomena related to climate change that inevitably affect the Cultural Heritage (CH). The pressures stressing the territorial dimension due to climatic changes lead to the decrease of essential resources and burden on the CH. To overcome the lack of information needed at various territorial scales, it becomes necessary to construct detailed and dynamic cognitive frameworks. This paper establishes a multitemporal information framework regarding the case study area, the Island of Santo Spirito in Venice, using several geomatic techniques to investigate the island's ecological significance and constructed heritage. The suggested methodology uses the integration of multitemporal data resulting from the processing of satellite images provided by the Copernicus satellites (Sentinel-2) and data from geomatic documentation techniques. Two separate methods were used in the survey operations: a Terrestrial Laser Scanning (TLS) and aerial photogrammetry from Uncrewed Aerial Vehicles (UAV) survey. The integration of satellite, aerial, and terrestrial data has allowed a complete knowledge of the necessary parameters for the monitoring of the CH of the area. In order to manage conservative policy from a preventive perspective and to recreate and digitally visualize missing historical phases, programmed monitoring is a crucial instrument.

## 1. INTRODUCTION

Cultural and Natural Heritage (CNH) arouse importance because of their sociocultural value, a value that is being jeopardized by the consequences caused by unexpected climatic events (Sevieri et al, 2020) and anthropogenic actions (Bonazza et al., 2022)

The current context leads to reflection about the consequences that climatic variations cause in these environments. The importance of CNH is highlighted by the activities that several relevant agencies have undertaken. Among these it is important to mention the UNESCO World Heritage and Sustainable Development Program which focuses on demonstrating the need for sustainable prevention and management of these areas (Xiao et al., 2018). CNH are also considered within the United Nation's Sustainable Goals (SDGs) particularly in SDG 11 "Make cities inclusive, safe, resilient and sustainable" (United Nations, 2015). Nationwide and across Europe, the study and knowledge of CNH require the development of multi-disciplinary and multi-scale methodologies for data recording, representation, and correlation from various platforms for the analysis of the state of the art, the knowledge, the control of the phenomena, and the preventive simulation of scenarios (Fabris, 2019). Due to the heterogeneity of the various geoDBs that are currently available (Mills et al., 2005), on-site validation and time monitoring are required to control the phenomena related to climate change that inevitably affect the CNH especially in complex environmental contexts like the coastal and marine.

There are many techniques that can be used to study territorial changes and consequently CNH changes involving different techniques and different spatial scales of application.

Continuous and differential global positioning systems, interferometry, satellite images, traditional topographic

measurements, repeated geometric leveling on benchmarks, light detection and ranging (LiDAR), airborne laser scanning (ALS), and aerial digital photogrammetry. Furthermore, unmanned aerial vehicle (UAV) and terrestrial laser scanning (TLS) systems (Rodríguez-González et al., 2017) can be used successfully in small areas. Aerial photogrammetry specifically offers the kind of continuous datasets required for multi-time monitoring and enables the reconstruction of various phenomena over extended time periods because of "historical" and continuous data. One of the most effective methods for determining a large number of points' coordinates from which high-resolution digital models and orthophotos can be derived is the digital photogrammetric method. In order to determine displacements and morphological changes, models with high resolution and precision that are repeatedly acquired throughout an area can be used to assess planimetric surface variations, mass movements, and structural collapses. An additional essential source of historical information are the accessible historical and photographic archives, which can be used to recreate old buildings and ground surfaces on a local scale.

Related to these approaches there are other techniques that involve larger areas of territory: the Earth Observation (EO) techniques. In recent years, the field related to EO has provided important opportunities for the implementation of monitoring and decision-aid systems. Current EO techniques (Pohl & Van, 1998; Bioucas-Dias et al., 2013) can be defined as an approach aimed at the study of land and the environment, which makes it possible to acquire detailed information on the qualitative and quantitative characteristics of surfaces and portions of land. In this way it is possible to formulate interpretative hypotheses about their state, changes, and the dynamic processes by which they are affected (Boschetti et al., 2006). The potential of EO

techniques has been used for studies inherent in territorial expansion and climatic factors (Bonazza et al., 2022) but at the same time studies have been pursued regarding the ecological and ecosystem values.

EO allows for a deeper understanding of the dynamics that distinguish climate phenomena, which originate impacts on territories, serving as a tool to support decision-making processes (Facchini et al., 2021).

This contribution describes a methodological approach through which in situ survey techniques can be integrated with EO data. The aim is to create a multi-temporal cognitive framework for the Venetian island of Santo Spirito, the case study of the work. The Venetian context characterised by the presence of countless examples of CNH lends itself as an interesting study area for the integration of in situ data with EO data. This method responds to a multidisciplinary approach that characterizes the study of the architectural heritage of the past where virtual reconstructions, if scientifically supported, can become clear and transmissible support decision tool. It is consequently necessary to understand how to manage the integration of different data (Croce et al., 2019), to evaluate the state of the built heritage and the resilience of natural areas by establishing multidisciplinary evaluation parameters.

The integration of these different types of data thus contributes to the construction of spatial knowledge frameworks used as a support tool and monitoring system for the stakeholders, belonging to different disciplines, involved in processes of protection and enhancement of the CNH.

### 1.1 Case study

With an approximate surface area of 550 km<sup>2</sup> and an average depth of 1 m, the Lagoon of Venice is the largest lagoon in the Mediterranean Sea. Its distinctive and sensitive environment is made up of a complex network of islands, canals, and lagoons. The islands of the lagoon are particularly susceptible to anthropogenic effects, such as pollution, urbanization, and tourism, as well as to natural changes, such as sea level rise, erosion, land subsidence, high tide.

The physical and ecological qualities of the lagoon have altered considerably in the previous century: the surface of the salt marshes has been decreased by 60%, and some portions of the lagoon are deepening due to a net sediment flux exiting from the inlets. The ecosystem of the lagoon may be significantly impacted by these changes at the inlets. Monitoring the CNH of the islands is therefore essential for their management and maintenance.

The Santo Spirito Island is specifically discussed; it is considered interesting for the following aspects: the value of the built environment in terms of history and culture, especially the church of Sansovino (Figure 1), which dates to the sixteenth century; the lack of detailed investigations into the minor islands of the Venetian lagoon; the island's state of neglect since 1965 that contributed to raising the area's criticalities, along with environmental and climate effects.

The island, which is situated in the southern lagoon between the islands of San Clemente and Poveglia, now resembles an abandoned building site, with the ruins of the outer wall that served as its protective barrier mixed in with those of the church and convent.



Figure 1. Aerial view of the Santo Spirito Island (2023, March).

## 2. MATERIALS AND METHODS

In order to investigate the island's ecological significance and constructed heritage and to comprehend their evolution, a temporal comparison between the monitored parameters was done in accordance with the goals established, using the three-year period between 2019 and 2023 as the reference period. Through two survey campaigns conducted during the target period, the research concentrated particularly on the integration of multitemporal data resulting from the processing of satellite images provided by the Copernicus satellites (Sentinel-2) and data from geomatic documentation techniques. Two separate methods were used in the survey operations: a TLS and aerial photogrammetry from UAV survey. A topographic Global Navigation Satellite System (GNSS) campaign enabled the acquired point clouds and elaboration to be georeferenced in the same reference system.

### 2.1 The 2019 survey campaign

The first campaign began in 2019. This survey's primary goal was not multitemporal monitoring, but rather comprehensive documentation of the current situation so that the historical stages that this island has experienced might be digitally reconstructed, together with the help of historical source research.

The survey activities have been planned because due to the extension and to the dense vegetation caused by the state of prolonged neglect, the acquisition of the entire island, as well as all the buildings and ruins, through the TLS would have required too many scans, moreover the state of instability and inaccessibility of some areas would have prevented a uniform sampling.

Given these presumptions, it was decided to focus the TLS survey on the church, performing internal and perimetral scans to also acquire the former convent complex partially and the 20th-century bunker. Using a FARO Focus 3D CAM2 S120 (Table 1), 20 external scans and 5 internal scans were acquired.

FARO Focus S120	Range [m]	Scanning frequency [points/sec]	Ranging error [mm]	FOV
	0.6 - 120	976000	±2	305°x360°

Table 1. Main specifications about the FARO Focus 3D CAM2 S120 laser scanner.

The FARO Scene Software (version 5.5.3.16)<sup>1</sup> was used for the LiDAR processing stage. Homologous points between the scans were selected, and the bundle was then optimized using the Iterative Closest Point (ICP) algorithm.

<sup>1</sup> <https://www.faro.com/it-IT/Products/Software/SCENE-Software>

A UAV was used to conduct aerial photogrammetry to map the entire island. With the exception of the bunker, which was entirely encircled by metallic armour, all buildings were also acquired by terrestrial photogrammetry.

Regarding the terrestrial photogrammetry, the exterior and interior of the Sansovinian church as well as the facades of the nineteenth-century farmhouse in the island's northeast and the "cavana" in the south were acquired. A boat circumnavigation of the island was done in order to collect the outer portion of the island walls, and photographs were taken at as frequent of intervals as possible. A Nikon D800 reflex camera (Table 2) mounted with a Nikon lens having a fixed focal length of 20 mm was used to take the photogrammetric images. The camera has a 36.3-megapixel CMOS FX sensor.

Nikon D800	Sensor size [mm]	Resolution	Focal length [mm]	Pixel size [ $\mu$ ]
	35.9x24	7360x4912	20*	4.8
* For the considered dataset				

**Table 2.** Nikon D800 main specification.

The DJI Mavic 2 Pro drone (Table 3), which is equipped with a Hasselblad L1D-20c camera with a 1" CMOS sensor, was used in the aerial photogrammetry phase.

Mavic 2 Pro	Sensor size [mm]	Resolution	Focal length [mm]	Pixel size [ $\mu$ ]
	13.2x8.8	5472x3648	10.26	2.4

**Table 3.** Mavic 2 Pro camera main specs.

During the survey, eight flights were scheduled and executed. Two flight plans for each building were executed at various heights and with different camera inclinations. The entire surface of the island was surveyed using some flight plans, differing by gripping patterns, altitude, and number of frames. Two flight plans followed a grid scheme to acquire the entire island: the first at an altitude of 40 m through the acquisition of 63 frames, the second at a lower altitude by capturing 219 frames. Then, two additional flights used a double grid scheme. Both nadiral and oblique images were acquired.

The Structure from Motion (SfM) software Agisoft Metashape (version 1.6.0)<sup>2</sup> was used to process the photogrammetric data according to the prescribed workflow in order to produce Digital Elevation Model (DEM) (Figure 2) and orthophotos of the island (Figure 3).

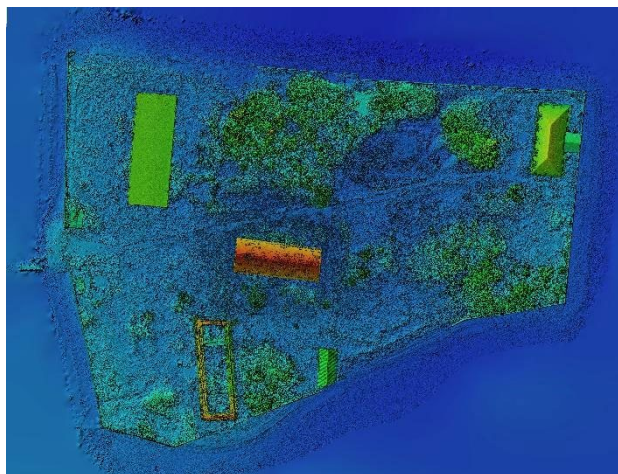


**Figure 2.** DEM of the island (2019 dataset).



**Figure 3.** Orthoimage of the island (2019 dataset).

Finally, the Topcon HiPer Pro GNSS (Global Navigation Satellite System) receiver was used to measure the 3D coordinates of 6 GCPs for the orientation of the final photogrammetric products. NRTK (Network Real-Time Kinematic) approach was used, and the platform was actively connected to the local GNSS permanent network. All of the point positions are expressed in terms of their coordinates using the Gauss-Boaga - Roma40 Fuso Est (EPSG 3004) reference system and geoidic elevation, which was calculated using ondulation made available by the Italian Geographic Military Institute (IGM). Due to the island's state of abandonment and the need to complete the survey quickly (tide variations make it difficult to land on the island for an extended period of time), GNSS acquisitions in static mode were not possible.

The main results of the acquisition and processing phase are reported in Table 4.

N° of images		N° of scans	N° of GCPs	RMSe LiDAR [cm]	RMSe SfM [cm]
Mavic 2PRO	Nikon D800	25	6	0.9	2.1
857	368				

**Table 4.** Principal results regarding the acquisition and the post-processing phase.

## 2.2 The 2023 survey

A second survey of the island was carried out in 2023 to meet the monitoring research goals.

Terrestrial Photogrammetric, UAV, LiDAR and GNSS data were acquired in the same way as the previous survey: 1138 photos and 16 scans were taken and a GNSS network of 5 points was created; as regards the instrumentation used, it varies slightly from the one used in 2019 (the Nikon Z7 camera and the STONEX® S900A receiver were used, instead of Nikon D800 camera and Topcon HiPer Pro), but remains equivalent in terms of accuracy and quality of the final data to allow an effective comparison between the two datasets. The main results of the acquisition phase, such as the main instrument specifications, are shown in Table 5 and Table 6.

Nikon Z7	Sensor size [mm]	Resolution	Focal length [mm]	Pixel size
	35.9x23.9	8256x5504	50*	4.35

<sup>2</sup> <https://www.agisoft.com/>

\* For the considered dataset

**Table 5.** Nikon Z7 main specification.

N° of images		N° of scans	N° of GCPs	RMSe LiDAR [cm]	RMSe SfM [cm]
Mavic 2PRO	Nikon Z7	16	5	0.4	1.3
760	378				

**Table 6.** Principal results regarding the acquisition and the post-processing phase.

The scans were then registered using the Cloud-to-Cloud (C2C) registration technique that was optimized with the ICP algorithm in Leica's Cyclone REGISTER 360 software<sup>3</sup>.

The image set was processed using the Structure from Motion (SfM) software Agisoft Metashape (version 2.0). The oriented scans were added to the structure from motion processing, blocking their alignment in a group and resetting the bundle external orientation.

Finally, the model was georeferenced through the use of the reference system and DEM (Figure 4) and orthophotos of the island (Figure 5) were produced. GNSS measured points in the Gauss-Boaga - Roma40 Fuso Est

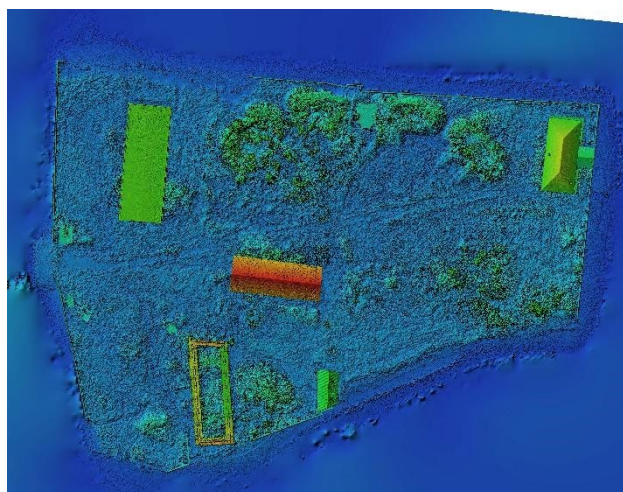


**Figure 4.** DEM of the island (2023 dataset).



**Figure 5.** Orthoimage of the island (2023 dataset).

The survey is of particular interest because in the target period, and before the actual completion of the MOSE system, there were exceptional tides that have affected Venice and all the islands of the lagoon. For example, in the particular case of the tide of 12 November 2019, the ground of the island of Santo Spirito was completely submerged. As was previously stated, the two datasets were created using similar instrumentations and the same acquisition strategy. For the purpose of monitoring, even if expeditious, the importance of having comparable data from the point of view of precision, accuracy and density is fundamental.

### 2.3 EO data: selection, bands combination and index computation

Once the study area on which to carry out the work was selected, the climate profiles covering the target years (2019 - 2022) were created, also considering the years included. The climate profiles provide an overall overview about the temperature trends in the study area, observing any anomalies that have occurred with the passage of time. From the bulletins provided by Arpa Veneto, average daily temperatures were extrapolated with reference to the years considered for the work. From the daily averages, monthly averages were calculated (Table 7).

	2019	2020	2021	2022
GEN	4.1	5.7	4.2	4.8
FEB	7.0	8.7	7.7	7.5
MA	10.3	10.0	9.4	8.9
R				
APR	13.9	14.6	12.0	12.6
MA	15.6	18.5	16.3	20.1
Y				
<u>JUN</u>	<u>25.5</u>	<u>21.6</u>	<u>24.3</u>	<u>25.2</u>
<u>JUL</u>	<u>25.8</u>	<u>24.6</u>	<u>25.0</u>	<u>27.6</u>
AUG	26.2	25.4	23.8	26.3
SEP	21.1	21.3	20.9	20.7
OCT	17.0	14.4	14.6	18.6
NOV	11.3	10.1	10.3	11.8
DEC	7.3	6.8	5.2	7.3

**Table 7.** Average monthly temperatures expressed in °C.

From the average temperatures, it is possible to observe a constant average climate trend for the time frame June 2019 - June 2022 and an increase for the time frame July 2019 - July 2022. The creation of climate profiles, in addition to a purely cognitive and framing purpose for the study areas, is also a prerequisite for the selection of satellite images. Days in the months of June and July were considered, in line with the detected climate trends, especially avoiding days with temperatures below the monthly average, to ensure the most truthful results possible.

To investigate and understand the changes occurred in the island, two Sentinel 2 images were acquired from the European Space Agency (ESA) Copernicus Open Access Hub one on July 20, 2019, and one on July 19, 2022.

In the present contribution direct segmentation of satellite images through indices was used (Zha et al., 2003). The calculation of indices is based on the absorption and reflection properties in different spectral bands of multispectral images.

The basis for the development of these indices is the spectral behavior that the ground has combined with the characteristics associated with the wavelengths of the electromagnetic spectrum in terms of absorption or reflection. Different bands of the satellite image represent different wavelengths of the

<sup>3</sup><https://leica-geosystems.com>

electromagnetic spectrum. Consequently, these indices were developed with a special combination of image bands (Table 8) (Bhatti et al., 2014).

Band	Name	Resolution	Index
8	NEAR	10 m	NDVI NDWI
4	RED	10 m	NDVI
3	GREEN	10 m	NDWI
8A	NEAR	20 m	NDBI
11	SWIR	20 m	NDBI

**Table 8.** Bands used and their characteristics in terms of type and spatial resolution.

### 2.3.1 Normalized Difference Vegetation Index (NDVI):

The NDVI is a widely used index for mapping the presence or absence of vegetation in each portion of land. It bases its operation on the unique shape of the vegetation reflectance curve (Zha et al., 2003). The NDVI index is expressed as the ratio of the difference to the sum of re-emitted near-infrared and red radiation; in fact, this index is calculated from visible and near-infrared light, which are reflected by vegetation. Healthy vegetation absorbs most of the visible light that strikes it and reflects most of the light in the near infrared. In the presence of diseased or sparse vegetation there will be more visible light reflection and less near-infrared light reflection. The formula for calculating the NDVI is:

$$NDVI = \frac{(NIR - RED)}{(NIR + RED)} \quad (1)$$

The near-infrared (NIR) band corresponds to band 8 in the Sentinel 2 mission. The red (RED) band corresponds to band 4. The NDVI value is between -1 (no vegetation) and 1 (presence of vegetation). Vegetation tends to absorb solar radiation by re-emitting some of it. Depending on the health and development status of the plant, the percentage of solar radiation that the plant emits may change.

### 2.3.2 Normalized Difference Built Up Index (NDBI):

Understanding the spatial distribution and growth of urban areas is an essential activity if a monitoring system is to be developed. One of the basic activities necessary for this purpose is the mapping of built-up areas. To map this phenomenon, it was decided to use the Normalized Difference Built-up Index, an indicator that describes the intensity of urban area development (Macarof et al., 2017). Similar to the calculation of the NDVI, the NDBI index is also the result of a ratio. In this case, the relation is between the difference and the sum of the SWIR and NIR bands, the short-wave infrared, and near-infrared bands, respectively.

$$NDBI = \frac{(SWIR - NIR)}{(SWIR + NIR)} \quad (2)$$

The SWIR band is number 11 for Sentinel 2. The NIR band corresponds to band 8. Standardized differentiation of these two bands will result in a value close to 0 for forest and agricultural land pixels, negative for water bodies, but positive values will be obtained for pixels containing built-up area, which allows these to be separated from other land covers (Zha et al., 2003).

### 2.3.3 Normalized Difference Water Index (NDWI):

The NDWI is an index used for mapping water bodies, which are characterized by low reflectance.

The bands used are the green band and the near-infrared band, which allow the spectral signatures of water-related entities to be identified, while eliminating soil and vegetation. NDWI is also used for turbidity analysis of waterways (Gao, 1996; McFeeters, 1996).

The formula for calculating the Normalized Difference Water Index is:

$$NDWI = \frac{(GREEN - NIR)}{(GREEN + NIR)} \quad (3)$$

$$NDWI = \frac{(GREEN - NIR)}{(GREEN + NIR)}$$

The green band is number 3 for Sentinel 2. As for the NIR band, this corresponds to band 8. The NDWI can take values between -1 and 1, and generally the value that the mapped water bodies take is above 0.5 (Kshetri, 2018).

### 2.3.4 Built Up Index (BUI):

The indices of NDBI and NDVI were further combined to obtain the BUI This index is based on a methodology developed by He et al. (2010) which refines the quality of processing that is obtained from calculating the simple NDBI.

The Built - up Index is expressed by the difference between the NDBI index and the NDVI index (He et al., 2010):

$$BUI = NDBI - NDVI \quad (4)$$

In opposition to the binary output of the original technique proposed by Zha, Gao and Ni (2003), in this case a continuous Built-Up image was produced through the approach developed by He et al (2010) in which a higher value of one pixel indicates a greater chance of indicating a built up area (Bhatti & Tripathi 2014).

## 3. DATASET EVALUATION AND RESULTS

As reported in previous chapters, heterogeneous historical and geomatic data have been collected and acquired in recent years. Analytical techniques used were also different and multidisciplinary in their application, so the results are reported below in different thematical chapter.

### 3.1 Historical reconstruction

Historical research has allowed the identification of a series of phases of the island, characterized by historical events and transformations of buildings, which have been modelled in order to document and transmit the time transformations of this place. As can be seen in Figure 6Figure , six main periods can be identified within the island history: (a) the construction and first restoration period; (b) the ownership of the island by the *Frati Minori* Congregation; (c) the ownership of the *Marina Militare*, following the Napoleonic deletion of the religious orders; (d) World War I period; (e) the abandonment period; (f) a second abandonment period, after the regeneration and renovation project failure.

The points clouds acquired in 2019 served as the basis for the modeling through Autodesk 3ds Max software<sup>4</sup> of the state of the island; for the previous phases a revision of the model was used based on historical/cartographic documents. Finally, through a frontal view the historical aspect of the island has been proposed within a current context, so as to recreate through an image, as

<sup>4</sup> <https://www.autodesk.it/products/3ds-max/free-trial>

this place could have been if nothing had been destroyed (Figure 7).

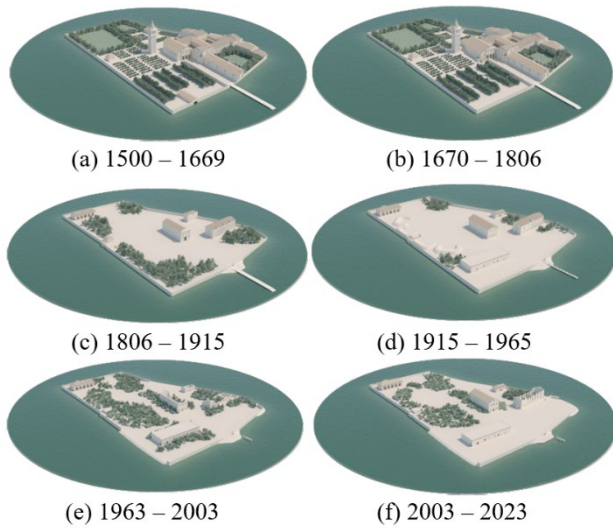


**Figure 6.** The six main historical phases of the Santo Spirito Island.



**Figure 7.** Hypothetical frontal view of the historical aspect of the Island within a current context.

### 3.2 Collapse analysis

To assess the deviations of the examined cloud using the root mean square error (RMSe), a C2C distance computing was performed. In this instance, C2C is used to precisely detect variations between two representations of the same object made at two distinct times, and as a result, to identify any collapse, failure, or displacement of the architectural CH as well as of the surrounding landscape.

In Figure 8, it can be seen the effects of the 5 days high tide occurred in November 2019: the outcome of the C2C comparison is depicted in the false color picture, which enables to hypothesize on several types of ongoing architectural disruptions and environmental change processes.

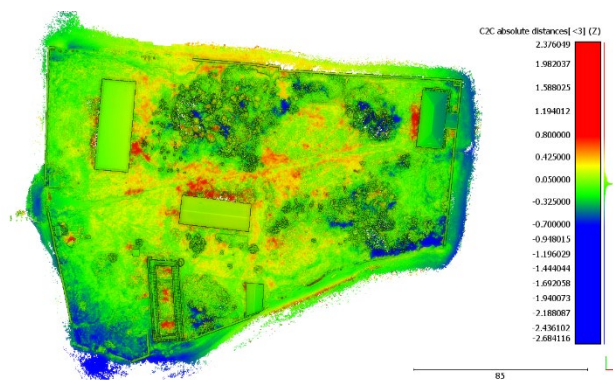


**Figure 8.** C2C comparison between the 2019 and 2023 datasets. The image shows in blue the eroded part of the island.

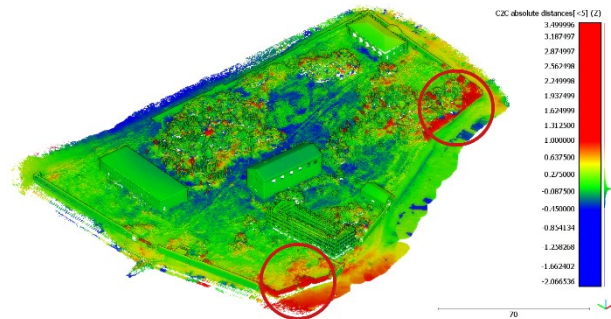


**Figure 9.** C2C comparison between the 2019 and 2023 datasets. The image shows in red the collapsed boundary walls.

During the five days of exceptionally high tide in November 2019 (and more generally all days of high tide during the period 2019–2023) a portion of the emerged land in the south part of the island was eroded by the floods (in blue color, about  $-0.5$  m), leading to a deposit in the northern zone (yellow/red, about  $+0.3$  m).

As for the damage to the architectural heritage, the comparison allows to identify the collapse of some parts of the boundary wall in the southern area of the island (Figure 9).

### 3.3 EO results and multi-temporal comparison

The combination of bands enabled the following outputs for the two target years, 2019 and 2022 through which a time comparison of the study area can be described.

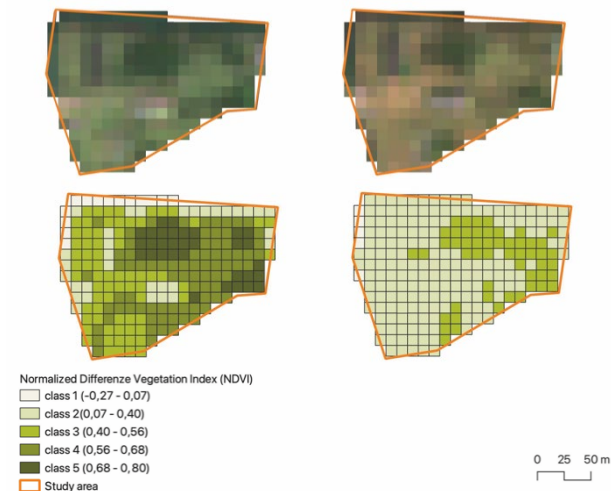


**Figure 10.** Result of NDVI in 2019 (left) and 2022 (right).

Mapping the vegetation of the study area shows a significant decrease in green area (Figure 10). By dividing the values of the mapped pixels into five classes (where class 1 is the lowest and class 5 the highest), it is possible to observe a variation regarding all five classes (Table 9). There is a decrease in the highest classes (class 4 and class 5) and a subsequent increase in the intermediate class (class 3). There is no change in land use and thus loss of green areas due to anthropogenic actions. This data, together with the prior knowledge possessed with respect to the study area, makes it possible to understand how the variation in vegetation, in the case of the island of Santo Spirito, is caused by climatic changes, which contribute to an increase in average temperature and a consequent variation in the phenological phases of the plant components of the area. This results in a delay in plant development or lower vigor due to adverse climatic conditions. For this reason, for both 2019 and 2022, it is possible to identify

areas that possess shrub and tree vegetation but are represented by very different NDVI values.

Class	Values	2019	2022
1	-0,27 -0,07	1400 m <sup>2</sup>	500 m <sup>2</sup>
2	0,07 - 0,4	3200 m <sup>2</sup>	5200 m <sup>2</sup>
3	0,4 – 0,56	7000 m <sup>2</sup>	16900 m <sup>2</sup>
4	0,56 – 0,68	7800 m <sup>2</sup>	0 m <sup>2</sup>
5	0,68 – 0,8	3200 m <sup>2</sup>	0 m <sup>2</sup>
tot		22600 m <sup>2</sup>	22600 m <sup>2</sup>

**Table 9.** NDVI variations in 2019 and 2022.

The area of Santo Spirito Island has not undergone any real changes in terms of the presence of water component (Figure 11). From the orthophotos and the study of the area that were taken into consideration, the presence of water bodies does not emerge.

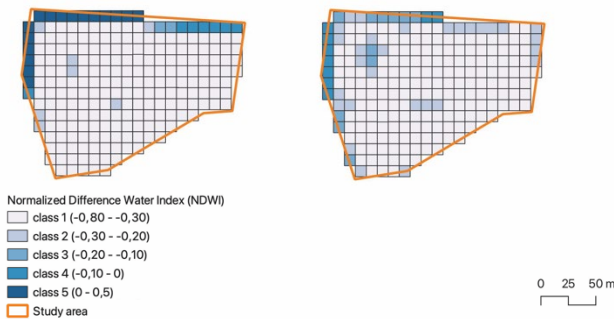


**Figure 11.** Result of NDWI in 2019 (left) and 2022 (right).

Thus, the two mappings related to the NDWI calculation performed for 2019 and 2022 record only slight changes in the pixel values (Table 10), which may be related to the lower presence of vegetation and the consequent lower evapotranspiration capacity.

Class	Values	2019	2022
1	-0,27 -0,07	1400 m <sup>2</sup>	500 m <sup>2</sup>
2	0,07 - 0,4	3200 m <sup>2</sup>	5200 m <sup>2</sup>
3	0,4 – 0,56	7000 m <sup>2</sup>	16900 m <sup>2</sup>
4	0,56 – 0,68	7800 m <sup>2</sup>	0 m <sup>2</sup>
5	0,68 – 0,8	3200 m <sup>2</sup>	0 m <sup>2</sup>
tot		22600 m <sup>2</sup>	22600 m <sup>2</sup>

**Table 10.** NDWI variations in 2019 and 2022.

The built-up index, which is the result of the difference between the normalized built-up index (NDBUI) and the NDVI, permits observing the presence of built-up areas within the study area and their possible increase or decrease.

The outputs obtained from the mappings carried out for 2019 and 2022 bring out how the study area has not undergone changes and new constructions as much as their abandonment and a gradual loss of vegetation component (Figure 12; Table 11).

Therefore, the volumes present have remained unchanged, while what can be observed is their decline in terms of their state of preservation, a fact that through in situ surveys can be appreciated in greater detail. In fact, the resolution that the bands allow for (in the case of the BUI it is 20 meters instead of 10) does not allow for a restitution of the index like the elaborations for the NDVI and NDWI but is limited to outlining a broad spatial framework.

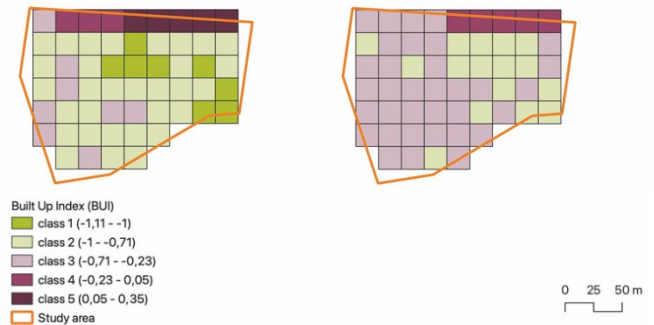


**Figure 12.** Result of BUI in 2019 (left) and 2022 (right).

Class	Values	2019	2022
1	-1 - -0,9	3200 m <sup>2</sup>	0 m <sup>2</sup>
2	-0,9 - -0,7	12400 m <sup>2</sup>	6400 m <sup>2</sup>
3	-0,7 - -0,2	3200 m <sup>2</sup>	13600 m <sup>2</sup>
4	-0,2 - 0,05	1200 m <sup>2</sup>	2000 m <sup>2</sup>
5	0,05 - 1	2000 m <sup>2</sup>	0 m <sup>2</sup>
tot		22000 m <sup>2</sup>	22000 m <sup>2</sup>

**Table 11.** BUI variations in 2019 and 2022.

#### 4. DISCUSSIONS AND CONCLUSIONS

This paper describes an approach that aims to integrate different techniques and scales of representation for the implementation of a support tool for monitoring system. Current climatic variations, together with human activities make it necessary to act from a new perspective, augmenting the information possessed through approaches and methods that are streamlined and dynamic. The proposed methodology therefore allows not only to expand what are the knowledge frameworks possessed for CNH but to renew them over time with clear and accessible approaches. The integration of different techniques and approaches proves to be crucial. In situ data enables first enables to generate metrically accurate and reliable digital twins. This allows to document a site status, analyzing criticalities and transformations, planning recovery and security measures. In situ data reliability also supports and verifies EO derived data and analysis, setting up as a ground truth for larger-scale analysis.

On the other hand, EO techniques make it possible to obtain information on distant and/or inaccessible territories, avoiding direct displacement and invasive actions. The distance factor allows a macro view of territories. EO allows to identify in a territory the peculiarities that the different surfaces possess. It should be pointed out, however, that there are areas, such as the case study described in this contribution, whose small extent makes it necessary to create a dataset from ground surveys, since even the satellite data with the best resolution (10 meters) does not allow to obtain detailed information. The adoption of data resulting from the integration of in situ data and EO data allow to have a complete knowledge of the most important parameters for monitoring the CNH in Santo Spirito Island. This kind of methodological approach contribute to the implementation of a decision support tool for local stakeholders and authorities, regarding issues of protection, prevention and monitoring of CNH in an island context.

## 5. ACKNOWLEDGEMENTS

Authors would like to thank Stefano Fiumicetti for the preliminary part of the historical research and for taking part to the 2019 survey campaign.

## 6. REFERENCES

- Bhatti, S. S., Tripathi, N. K., 2014. Built-up area extraction using Landsat 8 OLI imagery. *GIScience & Remote Sensing*, 51(4), 445-467.
- Bioucas-Dias, J. M., Plaza, A., Camps-Valls, G., Scheunders, P., Nasrabadi, N. M., & Chanussot, J., 2013. Hyperspectral remote sensing data analysis and future challenges. *IEEE Geoscience and Remote Sensing Magazine*, 1(2), 6-36.
- Bonazza, A., Bonora, N., Duke, B., Spizzichino, D., Recchia, A. P., & Taramelli, A., 2022. Copernicus in Support of Monitoring, Protection, and Management of Cultural and Natural Heritage. *Sustainability*, 14(5), 2501.
- Boschetti, M., Bolzan, L., Bresciani, M., Giardino, C., L'Astorina, A., Lanari, R., ... & Zilioli, E., 2006. Volume III Il Telerilevamento. In: *Collana Diffusione e sperimentazione della cartografia, del telerilevamento e dei sistemi informativi geografici come tecnologie didattiche applicate allo studio del territorio e dell'ambiente*.
- Croce, V., Caroti, G., Piemonte, A., & Bevilacqua, M. G., 2019. Geomatics for Cultural Heritage conservation: Integrated survey and 3D modeling. In *Proceedings of the IMEKO TC4 International Conference on Metrology for Archaeology and Cultural Heritage*, MetroArchaeo, Florence, Italy (pp. 4-6).
- Fabris M., 2019. Coastline evolution of the Po River Delta (Italy) by archival multi-temporal digital photogrammetry. *Journal: Geomatics, Natural Hazards and Risk*. Volume: 10 (1). Pages: 1007–1027. DOI: 10.1080/19475705.2018.1561528.
- Facchini, M., Taramelli, A., Bartoloni, A., Bernardi, M., Geraldini, S., Stortini, M., ... & Grandoni, D., 2021. Copernicus e le nuove frontiere per l'ambiente in *Ecoscienza – Sostenibilità e controllo ambientale* n. 5/2021.
- He, C., Shi, P., Xie, D., & Zhao, Y., 2010. Improving the normalized difference built-up index to map urban built-up areas using a semiautomatic segmentation approach. *Remote Sensing Letters*, 1(4), 213-221.
- Kshetri, T., 2018. Ndbi, ndbi & ndwi calculation using landsat 7, 8. *GeoWorld*, 2, 32-34.
- Macarof, P., Statescu, F., 2017. Comparison of ndbi and ndvi as indicators of surface urban heat island effect in landsat 8 imagery: A case study of Iasi. *Present Environment and Sustainable Development*, 11(2), 141-150.
- Mills, J.P., Buckley, S.J., Mitchell, H.L., Clarke, P.J. and Edwards, S.J., 2005. A geomatics data integration technique for coastal change monitoring. *Earth Surf. Process. Landforms*, 30: 651-664. <https://doi.org/10.1002/esp.1165>
- Pohl, C., Van Genderen, J. L., 1998. Review article multisensor image fusion in remote sensing: Concepts, methods and applications. *International Journal of Remote Sensing*, 19(5), 823-854.
- Rodríguez-González, P., Jiménez Fernández-Palacios, B., Muñoz-Nieto, Á., Arias-Sanchez, P., Gonzalez-Aguilera, D., 2017. Mobile LiDAR System: New Possibilities for the Documentation and Dissemination of Large Cultural Heritage Sites. *Remote Sensing* 9, 189. <https://doi.org/10.3390/rs9030189>.
- Sevieri, G., Galasso, C., D'Ayala, D., De Jesus, R., Oreta, A., Grio, M. E. D. A., & Ibabao, R., 2020. A multi-hazard risk prioritisation framework for cultural heritage assets. *Natural Hazards and Earth System Sciences*, 20(5), 1391-1414.
- United Nations, 2015. *Transforming Our World: The 2030 Agenda for Sustainable Development*. United Nations, Department of Economic and Social Affairs.
- Xiao, W., Mills, J., Guidi, G., Rodríguez-González, P., Barsanti, S. G., & González-Aguilera, D., 2018. Geoinformatics for the conservation and promotion of cultural heritage in support of the UN Sustainable Development Goals. *ISPRS Journal of Photogrammetry and Remote Sensing*, 142, 389-406.
- Zha, Y., Gao, J., Ni, S., 2003. Use of normalized difference built-up index in automatically mapping urban areas from TM imagery. *International journal of remote sensing*, 24(3), 583-594.